Hindawi Publishing Corporation
Journal of Nanomaterials
Volume 2013, Article ID 560542, 9 pages
http://dx.doi.org/10.1155/2013/560542

Research Article

Surface Modification on the Sputtering-Deposited ZnO Layer for ZnO-Based Schottky Diode

Ren-Hao Chang,[1] Kai-Chao Yang,[1] Tai-Hong Chen,[2] Li-Wen Lai,[2] Tsung-Hsin Lee,[3] Shiau-Lu Yao,[1] and Day-Shan Liu[1]

[1] *Institute of Electro-Optical and Material Science, National Formosa University, Yunlin 63201, Taiwan*
[2] *ITRI South, Industrial Technology Research Institute, Tainan 73445, Taiwan*
[3] *Metal Industries Research & Development Centre, Kaohsiung 81160, Taiwan*

Correspondence should be addressed to Day-Shan Liu; dsliu@nfu.edu.tw

Received 14 September 2013; Accepted 5 November 2013

Academic Editor: Liang-Wen Ji

We prepare a zinc oxide- (ZnO-) based Schottky diode constructed from the transparent cosputtered indium tin oxide- (ITO-) ZnO ohmic contact electrode and Ni/Au Schottky metal. After optimizing the ohmic contact property and removing the ion-bombardment damages using dilute HCl etching solution, the dilute hydrogen peroxide (H_2O_2) and ammonium sulfide $(NH_4)_2S_x$ solutions, respectively, are employed to modify the undoped ZnO layer surface. Both of the Schottky barrier heights with the ZnO layer surface treated by these two solutions, evaluated from the current-voltage (I-V) and capacitance-voltage (C-V) measurements, are remarkably enhanced as compared to the untreated ZnO-based Schottky diode. Through the X-ray photoelectron spectroscopy (XPS) and room-temperature photoluminescence (RTPL) investigations, the compensation effect as evidence of the increases in the O–H and O_{Zn} acceptor defects appearing on the ZnO layer surface after treating by the dilute H_2O_2 solution is responsible for the improvement of the ZnO-based Schottky diode. By contrast, the enhancement on the Schottky barrier height for the ZnO layer surface treated by using dilute $(NH_4)_2S_x$ solution is attributed to both the passivation and compensation effects originating from the formation of the Zn–S chemical bond and V_{Zn} acceptors.

1. Introduction

To accomplish a high-performance zinc oxide- (ZnO-) based optoelectronic device, the formation of a quality contact between ZnO and electrode is essential. A superior rectifying junction with metals and low-resistance ohmic contacts onto the ZnO surface is crucial to strengthen the diode application, UV detectors, gas sensors, piezoelectric transducers, and optical coatings [1–3]. Up to date, sputtering technology is a commonly used system for large-area and cost-efficiency ZnO-layered fabrication in application on the optoelectronic devices. However, limited reports on the ZnO-based Schottky diodes purely prepared using sputtering technology since significant defects formed in the films are inevitable due to the ion-bombardment damages and subsurface defects [4–6]. Accordingly, various ZnO surface passivation processes, such as chemical preparation with specific acid or organic solution, plasma bombardment, and activated light irradiation, were processed to achieve a quality ZnO-based Schottky diode [7–10]. Among the surface treatments, liquid-phase process, using the dilute hydrogen peroxide (H_2O_2) and ammonium sulfide ($(NH_4)_2S_x$) solutions, respectively, that has the simple and nonvacuum advantages over others, seems to be the best process method. Although reports had demonstrated that the improvement of the resulting metal/ZnO contact was attributed to the surface state passivation [11–13], the dominated mechanism responsible for these surface treatments still was indefinite. Except for engineering a quality ZnO/metal Schottky contact, the low-resistance contacts between ZnO and the electrode also are crucial. Although most ZnO-based optoelectronics use metal structures contact to n-type ZnO films with a low specific contact resistance, ρ_c, in the range of 10^{-5}~10^{-7} Ω-cm [14–16], the conversion efficiency between photons and electrons of the resulting optoelectronic devices is limited due to their opaque nature at the emission/absorption wavelengths. Accordingly, the

Table 1: Electrical properties of the annealed *i*-ZnO, and cosputtered ITO-ZnO and ITO films.

Sample	Concentration (/cm^3)	Mobility (cm/Vs)	Resistivity (Ω cm)
Annealed *i*-ZnO	-7.4×10^{15}	69.7	3.3×10^{2}
ITO	-5.5×10^{20}	10.7	1.1×10^{-3}
ITO-ZnO	-1.0×10^{21}	21.4	2.9×10^{-4}

transparent conductive oxide (TCO) film becomes a good candidate to be employed as an ohmic electrode with low light reabsorption [17, 18].

In this work, with the aim to achieve a quality ZnO-based Schottky diode, a homogeneity indium tin oxide- (ITO-) ZnO cosputtered film was deposited onto the undoped ZnO layer as an ohmic contact electrode, followed by the surface modification processes combined with the preetching process, using the diluted HCl solution, and the surface treatment, using the dilute H_2O_2 and $(NH_4)_2S_x$ solutions, respectively, on the undoped ZnO layer prior to the Ni/Au Schottky metal deposition. The mechanisms responsible for the improvement of the ZnO-based Schottky diode were comprehensively investigated by using the X-ray photoelectron spectroscopy (XPS) and room-temperature photoluminescence (RTPL) measurements.

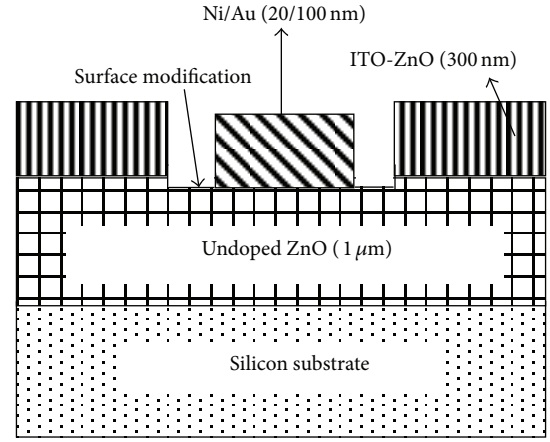

Figure 1: Schematic structure of the ZnO-based Schottky diodes.

2. Experiment

A 1 μm thick undoped ZnO (*i*-ZnO) layer was deposited onto the silicon substrate using a radio frequency (rf) magnetron cosputtering system. The undoped ZnO layer was subsequently annealed at 700°C for 30 min under oxygen ambient to improve the crystalline structure with *c*-axis growth orientation [10]. A homogeneity 300 nm thick ITO-ZnO cosputtered film at an atomic ratio of 33% [Zn/(Zn + In) at.%] was deposited onto the ZnO layer, followed by window of the ITO-ZnO film with a diameter of 300 μm which was completely eliminated using the dilute hydrochloric acid (HCl) solution for 40 sec. The residual ITO-ZnO/*i*-ZnO contact system was then optimized using an RTA treatment at 400°C for 1 min under vacuum ambient. After optimizing the ohmic contact electrode, the exposed ZnO layer surface was etched by the dilute HCl solution (referred as the preetching process hereafter) for 20 and 40 sec, respectively, to effectively remove the defects induced from the ion-bombardment damages during the cosputtered film deposition. Afterwards, the preetched ZnO layer surface was then, respectively, dipped in the dilute H_2O_2 solution at 100°C or dilute $(NH_4)_2S_x$ solution at 60°C for 3 min. Eventually, Ni/Au (20/100 nm) Schottky metal was deposited onto the surface-modified area with a diameter of 200 μm using e-beam evaporation, followed by liftoff using a standard photolithography technique. Figure 1 illustrates a schematic structure of the ZnO-based Schottky diodes.

Film thickness of the ZnO-based Schottky diode structure was measured using a surface profile system (Dektak 6 M). Carrier concentration and Hall mobility of these cosputtered films were measured using the Van der Pauw method (Ecopia HMS-5000) at room temperature. The radiation spectra and the chemical bond configurations near the undoped ZnO layer surface with and without the surface treatments were conducted from the photoluminescence (PL) spectra measured at room temperature using a He-Cd laser (λ = 325 nm) pumping source and characterized using an X-ray photoelectron spectroscopy (XPS, PHI Quantera SXM) with a monochromatic Al Kα source. Current-voltage (*I*-*V*) and capacitance-voltage (*C*-*V*) properties of the resulting Schottky diodes were characterized using a semiconductor parameter analyzer (HP4156C) and a LCR meter (HP4284A) at 1 MHz.

3. Results and Discussions

The electrical properties of the annealed undoped ZnO (*i*-ZnO) and cosputtered ITO-ZnO and ITO films are summarized in Table 1. Both the electron concentration and Hall mobility of the asdeposited cosputtered ITO-ZnO film were higher than those of the asdeposited ITO film, resulting in a low resistivity of 2.9×10^{-4} Ω cm [19]. The *I*-*V* characteristics of the asdeposited cosputtered ITO-ZnO and ITO films contact to the *i*-ZnO layer as well as the ITO-ZnO/*i*-ZnO contact system annealed at 400°C for 1 min under vacuum ambient using the transmission line method (TLM) are shown in Figure 2. All these contacts exhibited ohmic contact behavior. The transparent cosputtered ITO-ZnO film contact to the undoped ZnO layer resulted in a specific contact resistance (2.9×10^{-3} Ω cm^2) lower than that of the ITO film contact to the undoped ZnO layer (6.0×10^{-2} Ω cm^2). In addition, the specific contact resistance of the ITO-ZnO/*i*-ZnO contact system was further decreased to 4.6×10^{-5} Ω cm^2 after the RTA treatment. The mechanism responsible for the reduction

Table 2: Parameters of the Schottky diodes with and without an additive preetching process prior to the surface treatment using the dilute H_2O_2 solution.

Samples	Current ratio (@ ±2 V)	$\Phi_{B,I\text{-}V}$ (eV)	n
Nonetched	1035	0.68	1.45
Etched for 20 sec	6923	0.83	1.24
Etched for 40 sec	3.3×10^7	0.90	1.20

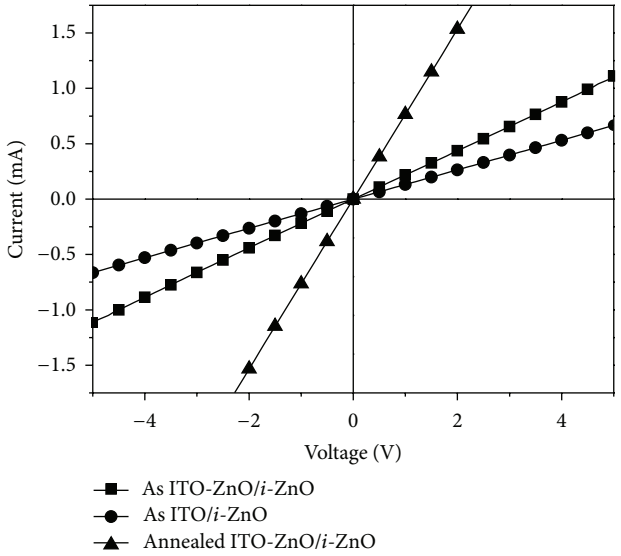

Figure 2: I-V characteristics of the asdeposited cosputtered ITO-ZnO and ITO films contact to the i-ZnO layer as well as the annealed ITO-ZnO/i-ZnO contact system.

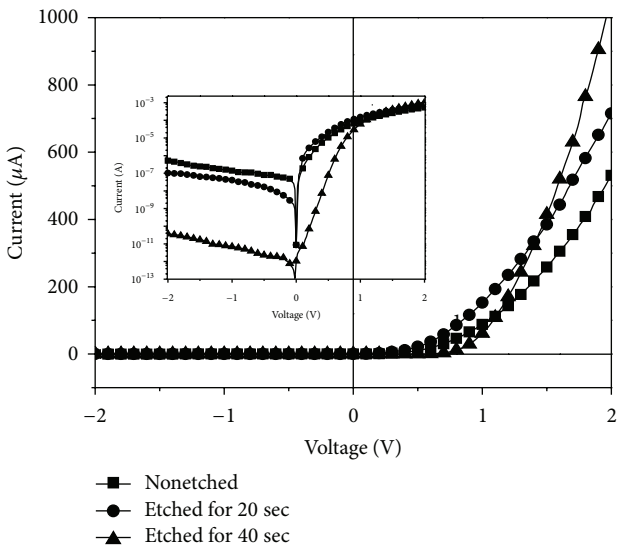

Figure 3: I-V characteristics of the ZnO layer contact to the Ni/Au metal with and without an additive preetching process prior to the surface treatment using the dilute HCl solution (the inset figure highlights the current in logarithmic scale).

in the contact resistance was ascribed to the interdiffusion between the ITO-ZnO/i-ZnO interfaces [20].

The I-V curve of the Ni/Au metal contact to the H_2O_2-treated ZnO layer without an additive preetching process using the dilute HCl solution is shown in Figure 3. The ZnO-based Schottky diode with the ZnO layer surface treated by dilute H_2O_2 solution showed rectifying behavior. The Schottky diode performance is evaluated by the forward current on the logarithmic scale, as shown in the inset figure, according to the thermionic theory:

$$I = I_s \exp\left[\left(\frac{q\left(V - \mathrm{IR_s}\right)}{nkT}\right) - 1\right], \tag{1}$$

where the saturation current, I_s, and ideality factor, n, of the Schottky diode indicated in (1) are determined as

$$I_s = AA^{**} \exp\left(-\frac{q\Phi_{B,I\text{-}V}}{kT}\right),$$
$$n = \frac{q}{kT}\left[\frac{dV}{d\left(\ln I\right)}\right], \tag{2}$$

where, the parameter q is the magnitude of electronic charge, k is the Boltzmann constant, T is the operating temperature, V is the applied forward bias, $\Phi_{B,I\text{-}V}$ is the Schottky barrier height (SBH), and A^* is the effective Richardson constant. In accordance with previous reports with an effective mass (m^*) of 0.27 m^0, the theoretical effective Richardson constant used to derive these Schottky diodes was 32 A cm^2 K^{-2} [21]. The derived parameters of the Schottky diode and the forward turn-on current to reverse leakage current ratio measured at 2 and −2 V, respectively, are listed in Table 2. Although the Schottky diode constructed from the Ni/Au metal contact to the H_2O_2-treated i-ZnO layer surface led to a barrier height of 0.68 eV and an ideality factor of 1.45, a low current ratio was obtained as a consequence of the high leakage current (~5×10^{-7} A), which is unfavorable for the Schottky diode application. Such apparent leakage current was attributed to the ion-bombardment damages on the ZnO layer during sputtering deposition. Accordingly, the preetching process using the dilute HCl solution was firstly carried out to remove the defects on the ZnO layer surface induced from the ion-bombardment damages during the cosputtered film deposition before the surface treatment on the ZnO layer using the dilute H_2O_2 solution. The resulting I-V characteristics of the ZnO layer surface contact to the Ni/Au metal with an additive preetching process for 20 and 40 sec prior to the surface treatment using the dilute H_2O_2 solution are shown in Figure 3 (the inset figure highlights the reverse current of these diodes in logarithmic scale). Evidently, the reverse current was significantly decreased to 3.64×10^{-11} A

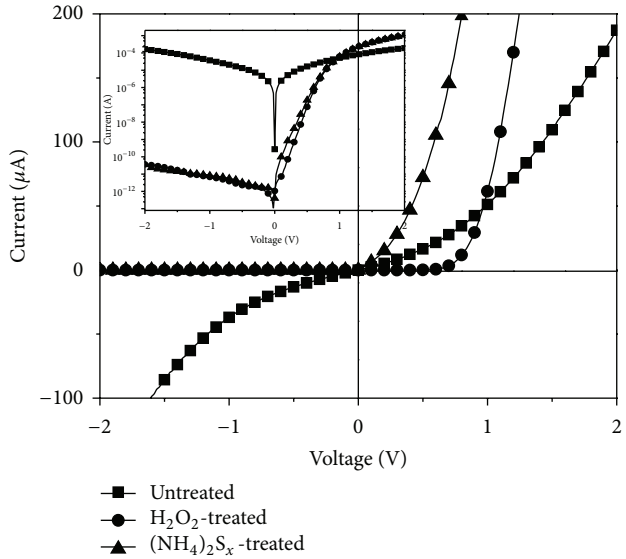

Figure 4: *I-V* curve of the ZnO layer contact to the Ni/Au metal with and without the surface treatments (the inset figure highlights the current in logarithmic scale).

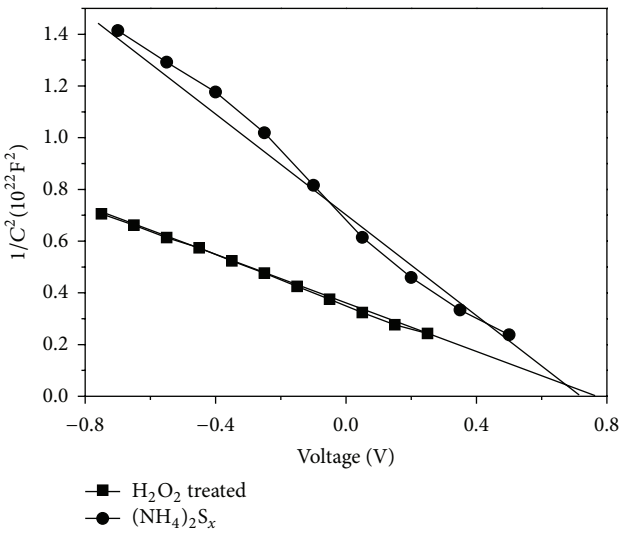

Figure 5: $1/C^2$ as a function of the applied voltage for the metallic Ni/Au contact to the surface-treated ZnO layer.

as the preetching process reached 40 sec, which also corresponded to a higher Schottky barrier height (0.90 eV) and ideality factor (1.20) as compared to the nonetched sample. This revealed that the additive preetching process on the *i*-ZnO layer prior to the surface treatment using the dilute H_2O_2 solution also was essential for further idealizing the sputtering-deposited ZnO-based Schottky diode.

Figure 4 gives the *I-V* curves of the metallic Ni/Au contact to the surface-treated ZnO layer, using dilute H_2O_2 and $(NH_4)_2S_x$ solutions, respectively, to study how these two surface treatments contributed to the Schottky diode performance (the Ni/Au contact to the untreated ZnO layer also is shown for comparison). It can be seen that the rectifying property of the Au/Ni/*i*-ZnO contact system was obviously improved using these two surface treatments. The device only etched by the dilute HCl solution (untreated sample) showed an almost symmetric *I-V* curve in the voltage range from −2 to 2 V, whereas the measured *I-V* characteristics of the Schottky diodes constructed for the H_2O_2- and $(NH_4)_2S_x$-treated ZnO layers exhibited the excellent rectifying behavior without significant breakdown at a reverse bias of −2 V. The leakage currents for both of the ZnO layer surfaces treated by using the dilute H_2O_2 and $(NH_4)_2S_x$ solutions, as shown in the inset figure, were apparently reduced from 0.16 mA to 3.64 pA and 3.28 pA, respectively. The derived barrier height, ideality factor, and forward turn-on current to reverse leakage current ratio of these three Schottky diodes by adopting the thermionic theory given in (1)–(3) are summarized in Table 3. The Schottky barrier high and ideality factors of the Ni/Au contact onto the untreated ZnO layer were 0.59 eV and 2.01, respectively, indicating that the preetching process still was insufficient for idealizing the Schottky contact property and multiple current pathways still existed in addition to thermionic emission. By contrast, the low reverse leakage current of the Ni/Au contact to the surface-treated ZnO layer led to a high current ratio of about 10^7, which also corresponded to a Schottky barrier height of approximately 0.9 eV, a value close to the ideal value (~0.85 eV), revealing that thermionic emission predominated the current transition. Figure 5 further illustrates the $1/C^2$ as a function of the applied voltage for the metallic Ni/Au contact to the surface-treated ZnO layer, using dilute H_2O_2 and $(NH_4)_2S_x$ solutions, respectively. The *C-V* relation for the ZnO-based Schottky diodes is described as [22]

$$\left(\frac{1}{C}\right)^2 = \left(\frac{2}{\varepsilon_s q N_d A^2}\right)\left(\frac{V_{\text{bi}} - V - kT}{q}\right), \tag{3}$$

where $\varepsilon_s = 9.0\,\varepsilon_0$ for ZnO [23], ε_0 is the permittivity in vacuum, N_d is the carrier concentration, A is the area of the Schottky contact, and V_{bi} is the built-in voltage. Accordingly, the carrier concentration and the built-in voltage are derived from the slope and intercept, respectively, of the curves shown in Figure 5. The carrier concentrations of 1.5×10^{15} and 2.1×10^{15} cm^{-3} were in turn calculated from the H_2O_2- and $(NH_4)_2S_x$-treated ZnO layer surfaces. Both of these values were significant lower than those of the untreated ZnO layer surface (6.9×10^{15} cm^{-3}), as shown in Table 3. In addition, the carrier concentration of the undoped ZnO layer surface etched by the dilute HCl solution for 40 sec also was calculated to be lower than that of the nonetched ZnO layer (7.4×10^{15} cm^{-3}), revealing that the preetching process was also beneficial for the reduction in the carrier concentration. The intercepts on the *x*-axis for the *C-V* curves of the H_2O_2- and $(NH_4)_2S_x$-treated Schottky diodes shown in Figure 5 were 0.76 and 0.71 V, respectively, whereas that of the Schottky diode without the surface treatment was 0.39 V (not shown).

Table 3: Parameters of the Schottky diodes with and without the surface treatments calculated from the I-V and C-V characteristics.

Samples	Current ratio (@ ±2 V)	$\Phi_{B,I\text{-}V}$ (eV)	n	$\Phi_{B,C\text{-}V}$ (eV)	N_d (/cm^3)
Untreated	1.15	0.59	2.01	0.66	-6.9×10^{15}
H_2O_2-treated	3.3×10^7	0.90	1.20	0.97	-1.5×10^{15}
$(NH_4)_2S_x$-treated	3.1×10^7	0.87	1.30	0.92	-2.2×10^{15}

The relationship between the Schottky barrier height ($q\Phi_B$) and the built-in voltage (qV_{bi}) is expressed as

$$q\Phi_{B,C\text{-}V} = q\left(V_{\text{bi}} + V_n\right),$$
$$V_n = \left(\frac{kT}{q}\right)\ln\left(\frac{N_c}{N_d}\right), \quad (4)$$

where V_n is the potential difference between the conduction band and the Fermi level of the undoped ZnO layer. N_c is the effective density of states in the conduction band of ZnO (~4.98×10^{18} cm^{-3}) [11]. The Schottky barrier heights of the Ni/Au contact to the ZnO layer surface treated by the surface treatment dilute H_2O_2 and $(NH_4)_2S_x$ solutions, respectively, were calculated to be 0.97 and 0.92 eV, as listed in Table 3. In addition, the ZnO layer surface only etched by using the dilute HCl solution resulted in a Schottky barrier height of 0.66 V while contacting to the Ni/Au metal. It also can be seen that the barrier heights derived from the I-V curves typical were lower than those calculated from the C-V characteristics. The difference in the Schottky barrier height between the I-V and C-V measurements was demonstrated to be the presence of the interface states which led to the image force barrier-lowering (IFBL) as derived from the I-V characteristics [11, 24]. Accordingly, the present surface modification processes, combined with the preetching process and the surface treatments using the dilute H_2O_2 and $(NH_4)_2S_x$ solutions, respectively, on the undoped ZnO layer were helpful to improve the resulting Schottky diode performance. The ion-bombardment damages on the sputtering-deposited ZnO layer were removed by an additive preetching process using the dilute HCl solution. By contrast, both of the surface treatments using the dilute H_2O_2 and $(NH_4)_2S_x$ solutions, respectively, were functional to significantly reduce the surface states on the ZnO layer surface, thereby improving the Schottky barrier height between the undoped ZnO layer and Ni/Au metal more effectively.

To further determine the improved mechanism of the Schottky diodes by these two surface treatments on the ZnO layer surface, using dilute H_2O_2 and $(NH_4)_2S_x$ solutions, respectively, the evolutions on the binding energies of the O 1s, Zn 2$p_{3/2}$, and S 2p core levels conducted from the XPS spectra were carried out. Figures 6(a) and 6(b), respectively, show the binding energy of the O 1s core level with and without the H_2O_2 surface treatment on the ZnO layer. It can be seen that the O 1s core level of the untreated ZnO surface exhibited a dominated peak of approximately 530.6 eV with a tail extending to high binding energy. This curve was deconvoluted into two overlapping peaks, located at 530.4 and 531.8 eV which were in turn associated with the O–Zn and O–H chemical bonds [25], by means of a combination of Gaussian and Lorentzian functions (70% Gaussian and 30% Lorentzian) with background subtraction. Different from the untreated sample, the intensity of the O–H chemical bond in the O 1s spectrum of the ZnO layer surface treated by dilute H_2O_2 solution apparently enhanced to result in a broad feature. Table 4 illustrates the composition of the O–Zn and O–H chemical bonds deconvoluted from the ZnO layer surface with and without the H_2O_2 surface treatment. The composition of the O–Zn chemical bond (59%) in

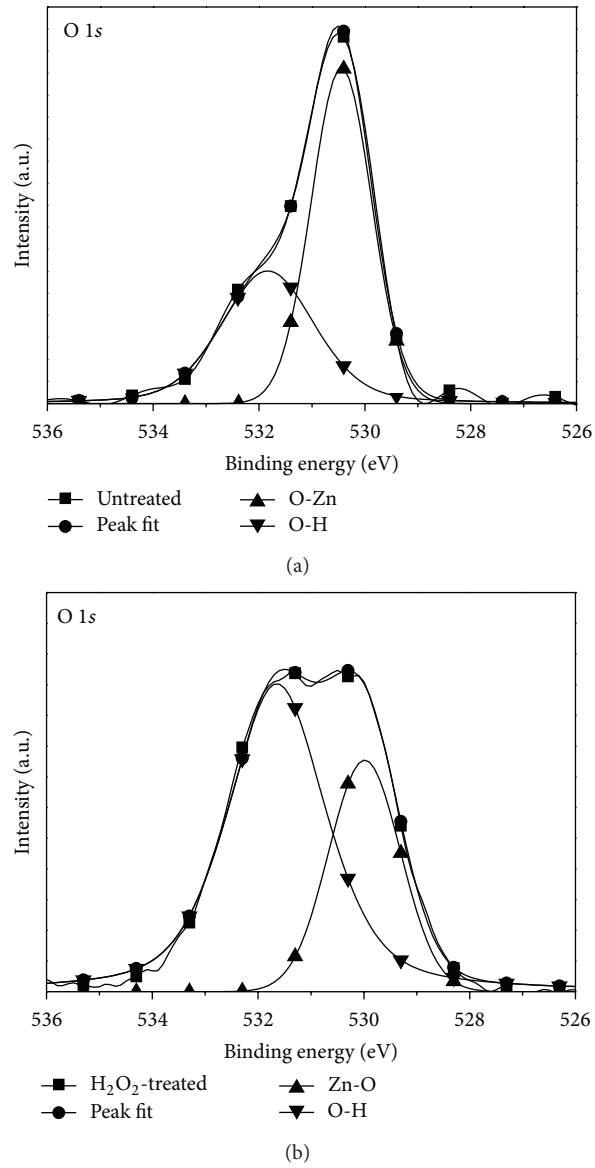

Figure 6: Binding energy of the O 1s core level for the (a) untreated and (b) H_2O_2-treated ZnO layer surfaces.

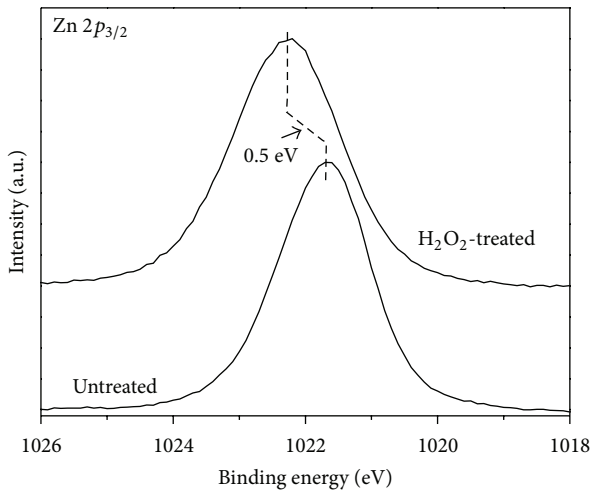

Figure 7: Binding energy of the Zn $2p_{3/2}$ core level for the untreated and H_2O_2-treated ZnO layer surfaces.

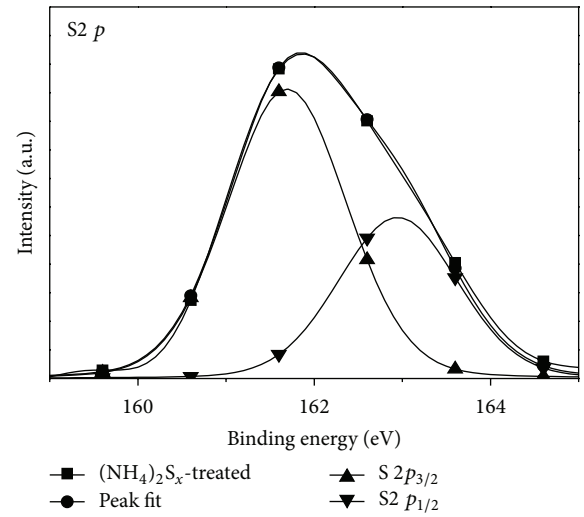

Figure 8: Binding energy of the S $2p$ core level for the $(NH_4)_2S_x$-treated ZnO layer surface.

Table 4: Compositions of the O–Zn and O–H chemical bonds for the untreated and H_2O_2-treated ZnO layer surfaces.

Samples	Untreated	H_2O_2-treated
O–Zn (%)	59	39
O–H (%)	41	61

Table 5: Compositions of the Zn–Zn, Zn–S, and Zn–O chemical bonds for the untreated and $(NH_4)_2S_x$-treated ZnO layer surfaces.

Samples	Untreated	$(NH_4)_2S_x$-treated
Zn–Zn (%)	30	4
Zn–S (%)	—	26
Zn–O (%)	70	70

the untreated ZnO layer surface was higher than that of the O–H chemical bond (41%), whereas the O–H chemical bond (61%) dominated over the H_2O_2-treated ZnO layer surface. The increase in the O–H chemical bond in the ZnO layer surface was closely related to the decomposition of the H_2O_2 solution. Since the O–H chemical bond is a well-known acceptor-like defect in the ZnO material [26], the Fermi level in the H_2O_2-treated ZnO layer surface was prone to be close to the vacuum level and thus led to the upward band bending. In addition, the red shift of the O–Zn (529.9 eV) and O–H (531.6 eV) binding energies after the H_2O_2-treated ZnO layer surface also gave evidence of the band bending of the ZnO layer surface [27]. The binding energies of the Zn $2p_{3/2}$ core level on the ZnO layer surface with and without the H_2O_2 treatment are shown in Figure 7. The binding energy of the Zn $2p_{3/2}$ core level in the untreated ZnO layer surface located at 1021.7 eV, a value lower than that of the bulk ZnO (1022.0 eV) owing to the native oxygen vacancies (V_o) formed in the sputtering-deposited ZnO layer [28]. For the ZnO layer treated by the dilute H_2O_2 solution, the V_o donors were compensated by the appearance of the O–H acceptors, thereby resulting in the blue shift of binding energy (~0.5 eV).

Figure 8 shows the S $2p$ core level of the ZnO layer surface treated by the dilute $(NH_4)_2S_x$ solution. A binding energy at 162.0 eV overlapped by the S $2p_{1/2}$ and S $2p_{3/2}$ with an interval of 1.2 eV was obtained from the $(NH_4)_2S_x$-treated ZnO layer surface, which was associated with the Zn–S chemical bond [29]. In addition, the binding energy located at 1021.7 eV of the Zn $2p_{3/2}$ core level for the untreated ZnO layer surface, as shown in Figure 9(a), was composed of two chemical bonds which in turn were denoted as Zn–Zn (1021.3 eV) and Zn–O (1021.8 eV). By contrast, the binding energy located at 1021.8 eV of the Zn $2p_{3/2}$ core level for the $(NH_4)_2S_x$-treated ZnO layer surface shown in Figure 9(b) was deconvoluted into three chemical bonds of Zn–Zn (1021.4 eV), Zn–S (1021.6 eV), and Zn–O (1022.0 eV), respectively [12]. The compositions in the ZnO layer surface with and without the $(NH_4)_2S_x$ treatment extracted from each area of the correspondent chemical bonds are summarized in Table 5. The composition of the Zn–Zn chemical bond (30%) which was linked to the V_o defects on the untreated ZnO layer surface had been effectively replaced by the appearance of the Zn-S chemical bond (26%), revealing that the ZnO layer surface treated by the dilute $(NH_4)_2S_x$ was favorable to passivate the formation of the V_o donors.

Figures 10(a)–10(c) show the RTPL spectra of the untreated and surface-treated ZnO layers. Two distinct emissions which in turn were denoted as the UV emission associated with near band edge emission (NBE) and the green-yellow emission associated with the deep level emission (DLE) were observed in these spectra. As given in these figures, the DLE emission was divided into several feature peaks of V_o (~2.11 eV), antisite oxygen (O_{Zn} ~ 2.38 eV), interstitial oxygen (O_i ~ 1.9 eV), and zinc vacancies (V_{Zn} ~ 2.72 eV), respectively [30–32]. The donor-related V_o emission dominated over the PL spectra of the untreated ZnO layer, whereas the acceptor-related O_{Zn} emission was the most intense peak in the H_2O_2-treated ZnO layer. From the XPS and RTPL measurements, the undoped ZnO layer surface

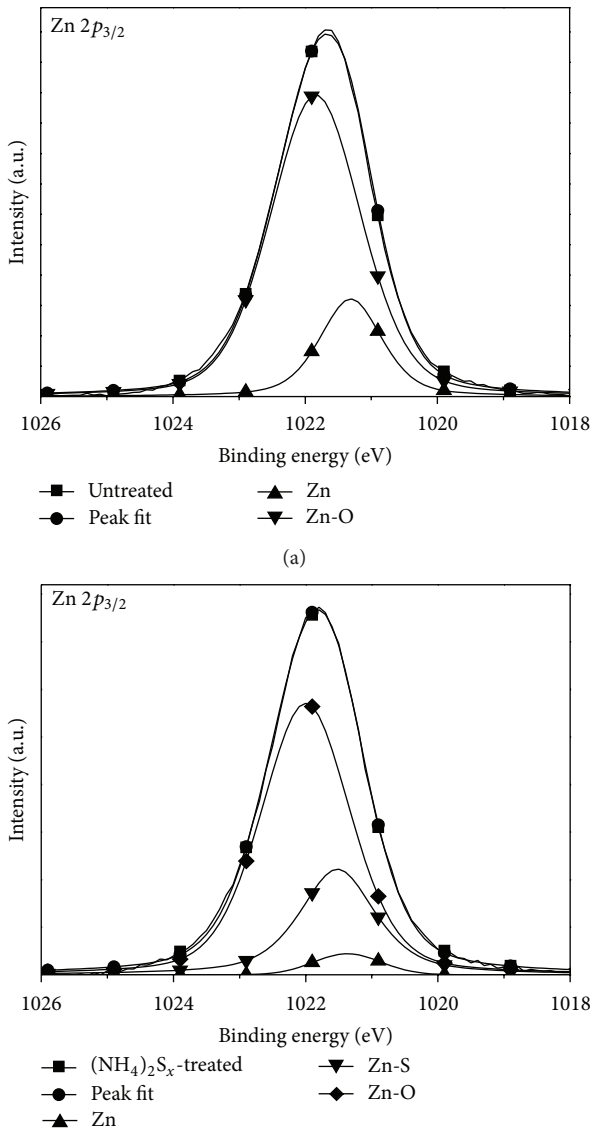

FIGURE 9: Binding energy of the Zn $2p_{3/2}$ core level for the (a) untreated and (b) $(NH_4)_2S_x$-treated ZnO layer surfaces.

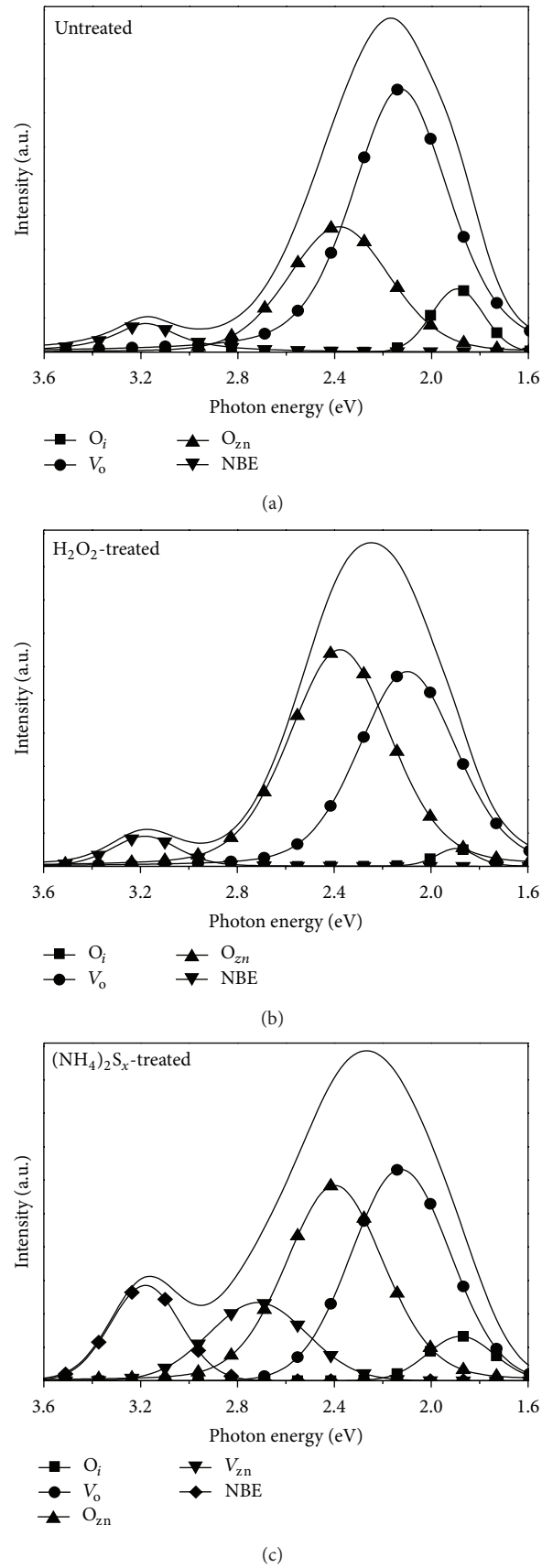

FIGURE 10: RTPL spectra of the (a) untreated, (b) H_2O_2-treated, and (c) $(NH_4)_2S_x$-treated ZnO layers.

treated by the dilute H_2O_2 solution thus was demonstrated to be beneficial for the enhancement on the O_{Zn} and O–H acceptors, which was functional to compensate the native V_o donors and even bring about the upward band bending of the ZnO layer surface, resulting in the increase in the Schottky barrier height. In contrast to the H_2O_2-treated sample, another deep level emission denoted as the V_{Zn} was observed in the RTPL spectra of the $(NH_4)_2S_x$-treated ZnO layer other than the apparent decrease in the V_o-related radiation compared to the untreated ZnO layer. Combined with the XPS and the RTPL measurements, the undoped ZnO layer surface treated by the dilute $(NH_4)_2S_x$ solution not only facilitated to suppress the formation of the V_o defects originating form to the formation of the Z–S chemical bonds but also induced the V_{Zn} acceptors, thereby causing the

reduction in the electron concentration on the ZnO layer surface and improving the contact behavior to the Ni/Au metal.

4. Conclusions

A quality ZnO-based Schottky diode was achieved using the transparent cosputtered ITO-ZnO ohmic electrode and Ni/Au Schottky metal. The homogeneity ITO-ZnO film deposited onto the undoped ZnO layer resulted in a low specific contact resistance of $4.6 \times 10^{-5}\,\Omega\,\text{cm}^2$ after an RTA treatment. In terms of the Schottky contact surface, an additive preetching process using the dilute HCl solution prior to the surface treatment on the undoped ZnO layer surface was crucial to remove the ion-bombardment damages during sputtering deposition. The increase in the Schottky barrier height between the ZnO and Ni/Au contact was found to be deeply correlated to the decrease in the carrier concentration of the ZnO layer surface modified by the combination process of the etching and the surface treatments, as derived from the *C*-*V* measurements. Accordingly, an optimal Schottky barrier height was obtainable from the undoped ZnO layer with the carrier concentration decreased from 7.4×10^{15} to $1.5 \times 10^{15}\,\text{cm}^{-3}$, which was etched by the dilute HCl solution and sequentially treated by the dilute H_2O_2 solution, contact to the Ni/Au metal. From the XPS and RTPL measurements, the mechanisms responsible for the enhancement on the Schottky barrier height of the H_2O_2-treated ZnO layer contact to Ni/Au were attributed to the compensation effect originating from the increase in the O-H and O_{Zn} acceptors. By contrast, the V_o donors passivation due to the formation of the Zn–S chemical bond and the compensation effect of the V_{Zn} acceptor formation in the ZnO layer treated by the dilute $(NH_4)_2S_x$ solution was the key factor to cause the improvement of the resulting Schottky diode performance. The transparent ZnO-based Schottky diode was fabricated from the surface-treated ZnO layer, using dilute H_2O_2 and $(NH_4)_2S_x$ solutions with an additive preetching process, thus exhibiting the high Schottky barrier heights of 0.90 and 0.87 eV, respectively.

Acknowledgments

The authors would like to acknowledge the support of National Science Council under Grant no NSC 102-2221-E-150-067 and the fund supports by ITRI South and MIRDC.

References

[1] B. N. Pal, J. Sun, B. J. Jung, E. Choi, A. G. Andreou, and H. E. Katz, "Pentacene-zinc oxide vertical diode with compatible grains and 15-MHz rectification," *Advanced Materials*, vol. 20, no. 5, pp. 1023–1028, 2008.

[2] O. A. Fouad, G. Glaspell, and M. S. El-Shall, "Structural, optical and gas sensing properties of ZnO, SnO_2 and ZTO nanostructures," *Nano*, vol. 5, no. 4, pp. 185–194, 2010.

[3] P. Reyes, J. Li, Z. Duan et al., "ZnO surface acoustic wave sensors built on zein-coated flexible food packages," *Sensor Letters*, vol. 11, no. 3, pp. 539–544, 2013.

[4] Y. Caglar, F. Yakuphanoglu, S. Ilican, and M. Caglar, "Electrical characterization of ZnO/organic semiconductor diode," *Journal of Optoelectronics and Advanced Materials*, vol. 10, no. 10, pp. 2584–2587, 2008.

[5] S. Chatterjee, A. K. Behera, A. Banerjee, L. C. Tribedi, T. Som, and P. Ayyub, "Nanometer-scale sharpening and surface roughening of ZnO nanorods by argon ion bombardment," *Applied Surface Science*, vol. 258, no. 18, pp. 7016–7020, 2012.

[6] R. F. Allah, T. Ben, D. Gonzalez, V. Hortelano, O. Martinez, and J. L. Plaza, "Modification of the optical and structural properties of ZnO nanowires by low-energy Ar^+ ion sputtering," *Nanoscale Research Letters*, vol. 8, article 162, 2013.

[7] J. D. Hwang, Y. L. Lin, and C. Y. Kung, "Enhancement of the Schottky barrier height of Au/ZnO nanocrystal by zinc vacancies using a hydrothermal seed layer," *Nanotechnology*, vol. 24, no. 11, Article ID 115709, 2013.

[8] J. Herran, I. Fernandez, R. Tena-Zaera, E. Ochoteco, G. Cabanero, and H. Grande, "Schottky diodes based on electrodeposited ZnO nanorod arrays for humidity sensing at room temperature," *Sensors and Actuators B*, vol. 174, pp. 274–278, 2012.

[9] B. Ryu, Y. T. Lee, K. H. Lee et al., "Photostable dynamic rectification of one-dimensional schottky diode circuits with a zno nanowire doped by H during passivation," *Nano Letters*, vol. 11, no. 10, pp. 4246–4250, 2011.

[10] B. T. Lai, C. T. Lee, J. D. Hong, S. L. Yao, and D. S. Liu, "Zinc oxide-based schottky diode prepared using radio-frequency magnetron cosputtering system," *Japanese Journal of Applied Physics*, vol. 49, Article ID 085501, 6 pages, 2010.

[11] M. S. Oh, D. K. Hwang, J. H. Lim, Y. S. Choi, and S. J. Park, "Improvement of Pt Schottky contacts to *n*-type ZnO by KrF excimer laser irradiation," *Applied Physics Letters*, vol. 91, no. 4, Article ID 042109, 2007.

[12] Y. J. Lin, S. S. Chang, H. C. Chang, and Y. C. Liu, "High-barrier rectifying contacts on undoped ZnO films with $(NH_4)_2S_x$ treatment owing to Fermi-level pinning," *Journal of Physics D*, vol. 42, no. 7, Article ID 075308, 2009.

[13] P. Singh, O. P. Sinha, R. Srivastava et al., "Surface modified ZnO nanoparticles: structure, photophysics, and its optoelectronic application," *Journal of Nanoparticle Research*, vol. 15, article 1758, 2013.

[14] H. Sheng, N. W. Emanetoglu, S. Muthukumar, B. V. Yakshinskiy, S. Feng, and Y. Lu, "Ta/Au ohmic contacts to n-type ZnO," *Journal of Electronic Materials*, vol. 32, no. 9, pp. 935–938, 2003.

[15] S.-H. Kim, K.-K. Kim, S.-J. Park, and T.-Y. Seong, "Thermally stable and low resistance Re/Ti/Au ohmic contacts to n-ZnO," *Journal of the Electrochemical Society*, vol. 152, no. 3, pp. G169–G172, 2005.

[16] J. L. Gu, Y. F. Lu, J. Zhang, L. X. Chen, and Z. Z. Ye, "Ti/Ni/Ti/Au Ohmic contact and Schottky transformation to Al-doped ZnO thin films," *Journal of Alloys and Compounds*, vol. 556, pp. 62–66, 2013.

[17] H. Y. Lee, C. T. Su, B. K. Wu, W. L. Xu, Y. J. Lin, and M. Y. Chem, "Fabrication and properties of indium tin oxide/ZnO schottky photodiode with hydrogen peroxide treatment," *Japanese Journal of Applied Physics*, vol. 50, Article ID 088004, 2 pages, 2011.

[18] H. W. Park, J. H. Bang, K. N. Hui, P. K. Song, W. S. Cheong, and B. S. Kang, "Characteristics of NiO-AZO thin films deposited by magnetron co-sputtering in an O_2 atmosphere," *Materials Letters*, vol. 74, pp. 30–32, 2012.

[19] D.-S. Liu, C.-S. Sheu, C.-T. Lee, and C.-H. Lin, "Thermal stability of indium tin oxide thin films co-sputtered with zinc oxide," *Thin Solid Films*, vol. 516, no. 10, pp. 3196–3203, 2008.

[20] C. C. Ho, L. W. Lai, C. T. Lee, K. C. Yang, B. T. Lai, and D. S. Liu, "Transparent cosputtered ITO-ZnO electrode ohmic contact to n-type ZnO for ZnO/GaN heterojunction light-emitting diode," *Journal of Physics D*, vol. 46, no. 31, Article ID 315102, 2013.

[21] M. W. Allen, X. Weng, J. M. Redwing et al., "Temperature-dependent properties of nearly ideal ZnO schottky diodes," *IEEE Transactions on Electron Devices*, vol. 56, no. 9, pp. 2160–2164, 2009.

[22] C. T. Lee, Y. J. Lin, and D. S. Liu, "Schottky barrier height and surface state density of Ni/Au contacts to$(NH_4)_2S_x$-treated *n*-type GaN," *Applied Physics Letters*, vol. 79, no. 16, article 2573, 2001.

[23] S. J. Young, L.-W. Ji, S. J. Chang, Y. P. Chen, and S.-M. Peng, "ZnO Schottky diodes with iridium contact electrodes," *Semiconductor Science and Technology*, vol. 23, no. 8, Article ID 085016, 2008.

[24] S. Lee, Y. Lee, D. Y. Kim, and T. W. Kang, "Impact of defect distribution on transport properties for Au/ZnO Schottky contacts formed with H_2O_2-treated unintentionally dopedn-type ZnO epilayers," *Applied Physics Letters*, vol. 96, no. 14, Article ID 142102, 2010.

[25] C. Li, H. Liang, J. Zhao et al., "Influence of high-pressure hydrogen treatment on structural and electrical properties of ZnO thin films," *Applied Surface Science*, vol. 256, no. 22, pp. 6770–6774, 2010.

[26] S. Liang, H. Sheng, Y. Liu, Z. Huo, Y. Lu, and H. Shen, "ZnO Schottky ultraviolet photodetectors," *Journal of Crystal Growth*, vol. 225, no. 2–4, pp. 110–113, 2001.

[27] J. O. Song, S. J. Park, and T. Y. Seong, "Effects of sulfur passivation on Ti/Al ohmic contacts to *n*-type GaN using CH_3 $CSNH_2$ solution," *Applied Physics Letters*, vol. 80, no. 17, article 3129, 2002.

[28] P. K. Kannan, R. Saraswathi, and J. B. B. Rayappan, "A highly sensitive humidity sensor based on DC reactive magnetron sputtered zinc oxide thin film," *Sensors and Actuators A*, vol. 164, no. 1-2, pp. 8–14, 2010.

[29] S. W. Shin, S. R. Kang, J. H. Yun et al., "Effect of different annealing conditions on the properties of chemically deposited ZnS thin films on ITO coated glass substrates," *Solar Energy Materials and Solar Cells*, vol. 95, no. 3, pp. 856–863, 2011.

[30] M. L. Cui, X. M. Wu, L. J. Zhuge, and Y. D. Meng, "Effects of annealing temperature on the structure and photoluminescence properties of ZnO films," *Vacuum*, vol. 81, no. 7, pp. 899–903, 2007.

[31] C. H. Tsai, C. I. Hung, C. F. Yang, and M. P. Houng, "Hydrogen peroxide treatment on ZnO substrates to investigate the characteristics of Pt and Pt oxide Schottky contacts," *Applied Surface Science*, vol. 257, no. 2, pp. 610–615, 2010.

[32] S. L. Yao, J. D. Hong, C. T. Lee, C. Y. Ho, and D. S. Liu, "Determination of activation behavior in annealed Al–N codoped ZnO Films," *Journal of Applied Physics*, vol. 109, no. 10, Article ID 103504, 2011.